

# Behavior of Piles subjected to Combined Axial and Lateral Loading

**Saja Saad Al-Amery**

Civil Engineering Department, College of Engineering, Mustansiriyah University, Baghdad, Iraq  
saja@uomustansiriyah.edu.iq (corresponding author)

**Mohammed Hussein Al-Dahlaki**

Civil Engineering Department, College of Engineering, Mustansiriyah University, Baghdad, Iraq  
mohammedhussein@uomustansiriyah.edu.iq

Received: 1 December 2024 | Revised: 23 December 2024 | Accepted: 11 January 2025

Licensed under a CC-BY 4.0 license | Copyright (c) by the authors | DOI: <https://doi.org/10.48084/etasr.9798>

## ABSTRACT

Pile foundations are employed to sustain both vertical and horizontal loads in various geotechnical applications, including coastal and offshore engineering. The contemporary design methodology analyzes the response of piles under combined horizontal and vertical loads independently and then superimposes them. This simple analytical method does not account for the combined loads' coupling effect. The number of studies on this subject is limited and the findings thus far are unclear about the effect of vertical loads on the lateral response of piles. In this paper, a number of model experiments were performed under different load conditions using the particle image velocimetry technique in well-graded sandy soil with a relative density of 65%. The results indicate that the presence of a low vertical load improves the lateral behavior of piles with L/D ratio (20, 25) due to the soil densification effect, and when the vertical load becomes 60 and 80% it results in a declining of the pile's lateral capacity. In piles with L/D ratio equal to 30, the P-Δ effect is more significant than the soil densification impact, which produces more pile deformation. This study also discusses the lateral displacement along the pile shaft using the PIV technique.

*Keywords-pile foundation; laterally loaded pile; combined loading effects; PIV technique*

## I. INTRODUCTION

A wide range of structures constructed on soft or loose soils are supported by pile foundations, as shallow foundations are prone to significant settlement or possess insufficient bearing capacity. These piles can support not only vertical loads, but also lateral loads or combinations of lateral and vertical loads. Numerous conditions, such as earthquakes, powerful winds, wave action, vessel collisions, liquefaction, and slope failure, can generate lateral loads. According to modern practice, the piles are usually analyzed separately to assess bearing capacity and settlement for vertical load and to evaluate flexural behavior for lateral load. This method is only effective with slight horizontal loads. In coastal and offshore regions, where horizontal loads can reach 10%–20% of vertical loads, examining the combined vertical and lateral load interaction effects is crucial and requires a methodical approach. The combined effect of vertical and lateral loads has not been thoroughly investigated.

The existing literature provides inadequate information, resulting in inconsistent findings on how piles' horizontal behavior is affected by vertical loads. Several studies have investigated the effect of vertical loads on the lateral response of piles to lateral loads. Numerical analysis and model testing have been utilized to investigate this phenomenon. Some

researchers have demonstrated that vertical loads enhance the lateral performance of piles [1-3]. Conversely, additional research has demonstrated that vertical loads decrease the lateral bearing capacity of piles [4, 5]. The influence of numerous factors, such as pile rigidity [6, 7], load application sequence [8, 9], and soil properties [10, 11] can determine the impact of vertical loads on the lateral behavior. Therefore, the underlying cause-and-effect process needs to be clarified to assess accurately the vertical loads' impact on piles' lateral response. Many researchers have addressed the issue of vertical and horizontal loadings by employing experimental testing conducted at full and small scales [12-19], experimental studies involving the use of a centrifuge model [20], and analytical models and numerical simulations [21-24].

Particle Image Velocimetry (PIV) is a non-intrusive optical measurement method employed to visualize and quantify fluid dynamics or material displacement. PIV, when utilized in the analysis of laterally loaded piles, offers significant insights into soil-pile interaction by documenting the deformation and displacement of soil particles surrounding the pile under lateral loading conditions. PIV is employed to quantify pile deflection behavior along the pile shaft and the transmission of lateral loads from the pile to the adjacent soil [25-28].

II. MATERIALS AND METHODS

A. Materials

The soil used for all models' tests is dry, clean sand sourced from a local construction material agent. Prior testing, the sand was air dried in a laboratory and was then sieved using a No. 2 sieve to remove large particles and any undesirable materials. Standard laboratory experiments were carried out to determine its physical characteristics. The physical parameters of the examined sand are summarized in Table I. The results (Figure 1) demonstrate that the sand is classified as well-graded sand (SW) according to the Unified Soil Classification System (USCS).

TABLE I. PHYSICAL AND SHEAR PROPERTIES OF THE USED SANDY SOIL

Index property	Value	Standard
Effective size, (mm)		
D10,	0.11	ASTM D 2487 [29] and ASTM D 422 (2006) [30]
D30,	0.4	
D60	0.85	
Coefficient of uniformity ( $C_u$ )	7.73	
Coefficient of curvature ( $C_c$ )	1.71	
Specific gravity ( $G_s$ )	2.67	ASTM D 854 (2006) [31]
Max. unit weight ( $kN/m^3$ )	17.46	ASTM D 4254 - (2006) [32]
Min. unit weight ( $kN/m^3$ )	16.2	ASTM D 4253 - (2006) [33]
Max. void ratio	0.616	-----
Min. void ratio	0.5	-----
Relative density (RD)%	65	-----
Unit weight $\gamma_d$ ( $kN/ m^3$ )	17	-----
Void ratio	0.54	-----
Internal friction angle $\phi$ ( $^\circ$ ) (direct shear test)	$36.6^\circ \approx 37^\circ$	ASTM D3080- 11 [34]
Internal friction angle $\phi$ ( $^\circ$ ) (triaxial test)	$36.8^\circ \approx 37^\circ$	ASTM-D7181-20 [35]

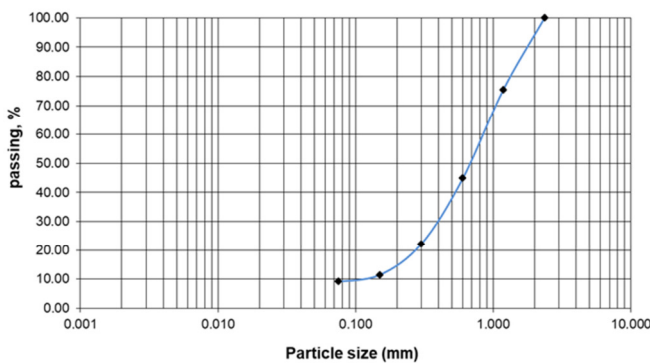


Fig. 1. Grain size distribution of the sandy soil.

B. Pile Models and Experimental Steel Box

In the current research, hollow aluminum half square piles with closed ends and a cross section of  $20 \times 10$  mm were used in all models with 1 mm wall thickness, 70 GPa, Young's modulus, and  $0.0025 \times 10^{-6} m^4$  moment of inertia. To prevent sand intrusion, the piles were sealed with silicone sealant. The pile models were produced with three distinct length-to-diameter ratios ( $L/D$ ), specifically 20, 25, and 30, considered as

short, intermediate, and long piles, respectively [36]. It is worth noting that the loads in all curves represent the double of the applied loads (because half pile-section was installed in the model). The pile cap utilized for the pile head is a well-made steel plate with dimensions of  $250 \text{ mm} \times 150 \text{ mm} \times 3 \text{ mm}$ . Choosing materials that closely mimic the properties of the soil and pile materials used in full-scale applications is crucial. For example, using natural sands with similar particle size distributions can help replicate the behavior of real soil conditions more accurately.

The experimental system comprises a rectangular box with dimensions of 750 mm length, 250 mm width, and 800 mm depth. The box was manufactured using 3 mm-thick steel plates for its base, two sides, and backside. The front side of the box was made of a 19-mm-thick glass sheet, as depicted in Figure 2. The thick glass was needed to prevent any buckling of the front side during tests.

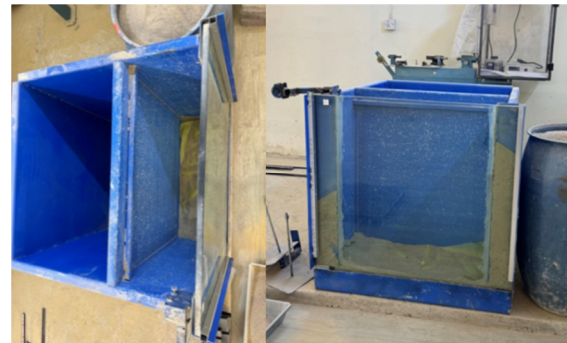


Fig. 2. Experimental steel box.

C. Particle Image Velocimetry Camera

The camera utilized in the present study is the Nikon D5200, a digital SLR camera with a resolution of  $6000 \times 4000$ . The camera was linked to a laptop for storing the captured photos, which were subsequently analyzed using the PIV approach for determine the lateral deformation along the pile shaft (Figure 3).



Fig. 3. PIV camera system.

III. TEST PROCEDURE

A. Soil Preparation

An essential aspect of the PIV technique is the inclusion of colorful targets that correspond to the movement of the soil matrix. These targets are captured through sequential

photography to track their motion. To achieve this, 20% of the initial soil amount used in the models was dyed with black ink and thoroughly mixed with the remaining soil required to fill the container. As earlier mentioned, the sand used in this study has a relative density of 65%, indicating medium-density. However, before sand placing, the container was partitioned into layers of equal heights using remark lines, extending all the way to the top of the box. Each layer has an even thickness of 10 cm. The particular relative density was accomplished by performing uniform distributed blows with a steel hammer after placing the predetermined weight of soil. A precision ruler with a sharp edge was then utilized to achieve the closest proximity level surface.

### B. Pile Installation and Dial Gages

To begin preparing the model, the first step was to vertically install the pile. Following that, the soil was prepared to achieve a certain density. Steel clamps were utilized for pile setting. The clamp serves the purpose of ensuring that the pile was aligned vertically and securely fixed to the side and upper surface of the box. To verify the vertical alignment of the pile, a measuring tool was used. To eliminate the friction between the pile shaft face (one side in contact with the Perspex glass sheet), lubricating oil was applied along one side of the pile shaft. This step is necessary to prevent any entrance of sand particles between the pile and the glass sheet. Finally, after soil preparation and placing into the steel box, the upper surface was leveled. Then, two dial gauges with a precision of 0.01 mm were placed at pile cap to measure the vertical and lateral movements of the pile head during the test time. The gauges were held in place using a magnetic stand base positioned opposite the cap of the pile.

### C. Compression and Lateral Loading Tests

Once the pile-loading test instrument was prepared and the pile was installed in the designated sand at the specified penetration depth, a PIV camera was positioned in a suitable location to capture photos of each load increment. Subsequently, static compression tests, static lateral load tests, and combined load tests were conducted for each considered L/D ratio. The static compression loading tests were conducted in accordance with the ASTM D1143-1994 [37] standard for vertical loading tests. The load was applied by incrementally increasing dead weights onto the pile cap until the pile failed, as shown in Figure 4. The tests for static lateral loading were carried out accordance with the ASTM D3966-1990 [38] standard for lateral loading tests. The lateral load was exerted on the pile using a weir, which was attached to the pile cap on one side and to the loading base on the other side through a pulley arrangement. The lateral load was gradually applied using dead load until the displacement reached 20 mm, which is equivalent to the diameter of the pile, as shown in Figure 5.

Vertical and lateral weights were applied together in two stages. Initially, vertical loads were imposed, followed by the application of lateral loads in the subsequent step, while maintaining a constant vertical load. The pile was exposed to a vertical load in four stages, with each stage representing 25% of the total vertical ultimate carrying capacity of the pile. Subsequently, the lateral load was applied as shown in Figure 6(a). The pile head settlement of the compression test and the

lateral displacement of the pile head were measured with dial gauges for each load increment. A picture for each load increment was taken, as shown in Figure 6(b).



Fig. 4. Vertical load test.



Fig. 5. Lateral load test.

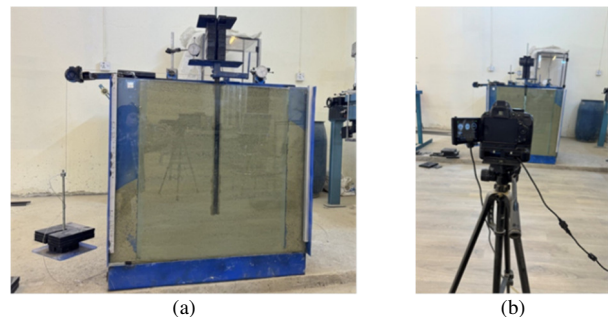


Fig. 6. (a) Combined load test, (b) PIV camera used.

## IV. RESULTS AND DISCUSSION

### A. Ultimate Axial Load Capacity Estimation

Figure 7 depicts the correlation between the vertical load capacity and the settlement measured at the pile head.

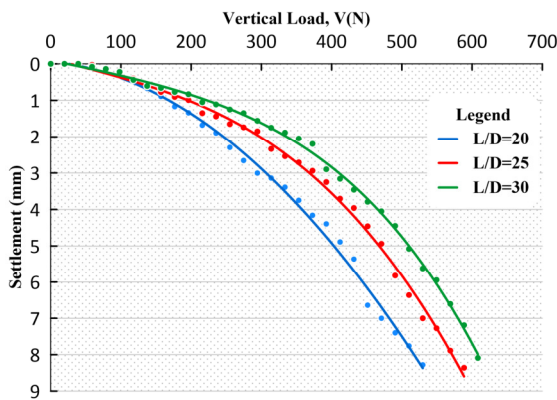


Fig. 7. Load-settlement curve for the axial pile load test.

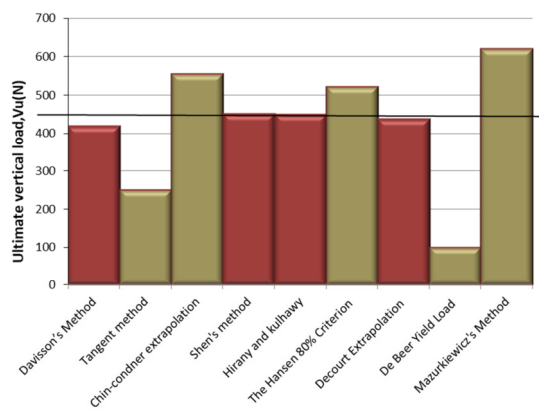


Fig. 8. Methods of Vult estimation for piles with L/D=20.

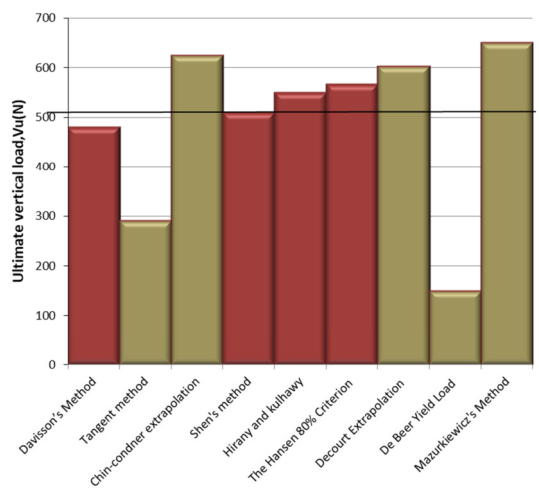


Fig. 9. Methods of Vult estimation for piles with L/D=25.

The assessment of the ultimate capacity or failure load of the pile requires the application of a precise criterion based on the analysis of load-settlement data received during testing. Historically, many methodologies have been proposed for assessing the ultimate capacity of axially loaded piles. The methods used to assess the ultimate resistance demonstrated by the tested piles are Davison's Method (1972), Tangent

method, Chin-condner extrapolation (1970), Shen's method (1980), Hirany and kulhawy (1989), Hansen 80% criterion (1963), Decourt extrapolation (1999), De Beer Yield Load (1968), and Mazurkiewicz's Method (1972) [34-36]. Figures 8-10 clarify the ultimate vertical loads (Vult) gradient using the above mentioned methods.

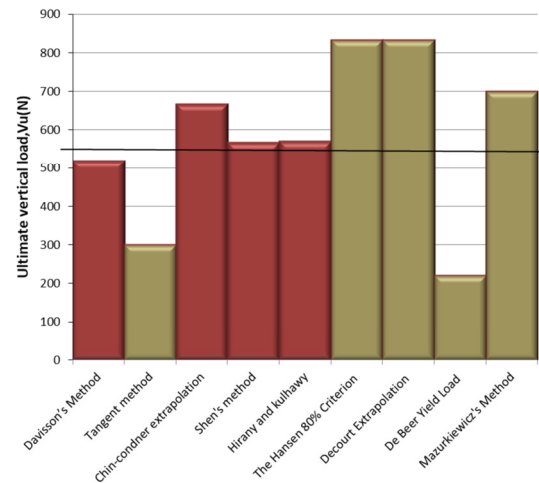


Fig. 10. Methods of Vult estimation for piles with L/D=30.

**B. Ultimate Lateral Load Capacity Estimation**

The techniques used in this work to evaluate the test results from lateral load tests in order to calculate the failure load rely on the structure's allowable displacement that the piles are supporting. Typically, the recognized criteria for assessing the ultimate lateral force are the failure load criterion (the failure load is defined as the load at which the tangents on the load-movement curve intersect) and the lateral displacement criterion (a failure load measured at a lateral displacement or deformation of 6.25 mm) [41]. Table II presents the ultimate lateral load (Hult) for the pile. It is evident that the value of (Hult) for a pile with L/D = 25 and 30 is higher than that of L/D = 20 by approximately 14.51% and 44.54%, respectively.

TABLE II. OBSERVED AND INTERPRETED Hult VALUES FOR A SINGLE PILE

Embedded length of pile (mm)	L/D	Observed pile lateral load at test end (N)	Interpreted Hult (N)		Adopted Hult (N)
			Intersection method	Load at 6.25 mm displacement	
400	20	568.98	375	258.4	258.4
500	25	647.46	400	295.9	295.9
600	30	745.56	525	373.5	373.5

Three values of the L/D ratio were investigated in order to clarify how it affects the horizontal displacement experienced at the pile head. The relationship between the lateral load capacity and the horizontal displacement produced at the pile is depicted in Figure 11, which represents measurements taken at the top of the pile. It should be noted that the test halted when the lateral displacement reached roughly 20 mm, which is equal to the width of the pile. It is evident that as the L/D ratio increases, the lateral load value also increases. This can be

attributed to the enlargement of the skin friction area during soil movement between the pile shaft and the surrounding soil results in an increase in soil resistance thrust, which helps to withstand the applied lateral load. Similar behavior was noted by other researchers, e.g. [37-39].

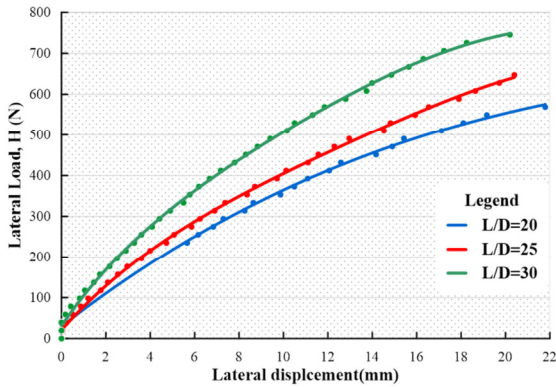


Fig. 11. Lateral load vs. displacement curves.

C. Piles Subjected to Combined Lateral and Axial Loads

Accordingly, to examine how the model piles behave when subjected to both lateral and vertical loads, the effects of applying vertical loads of 20% Vult, 40% Vult, 60% Vult, and 80% Vult were examined.

1) Influence of Vertical Load on the Lateral Response of the Pile

Figures 12-14 illustrate the effect of vertical load on the lateral behavior of piles for L/D equal to 20, 25, and 30.

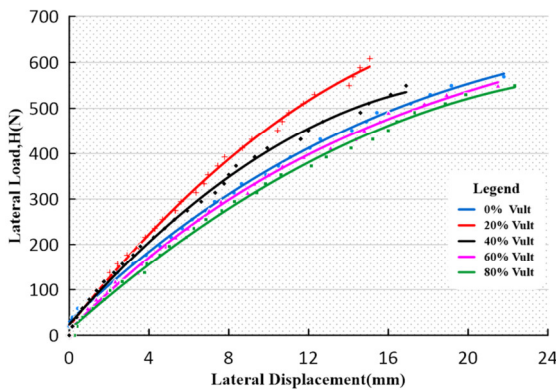


Fig. 12. Lateral load vs. lateral displacement curves for L/D=20.

For piles exposed to both lateral and axial loads, the results demonstrate that when the slenderness ratio is between 20 and 25 (short to intermediate pile), there is an increase in the lateral capacity of the piles when low percentage vertical loads (20% Vult) are present. This phenomenon is attributed to the increase in soil stiffness induced by vertical loads, known as the soil densification effect. In other words, soil densification resulting from the applied vertical loads reduces the pile's horizontal displacement and bending moment.

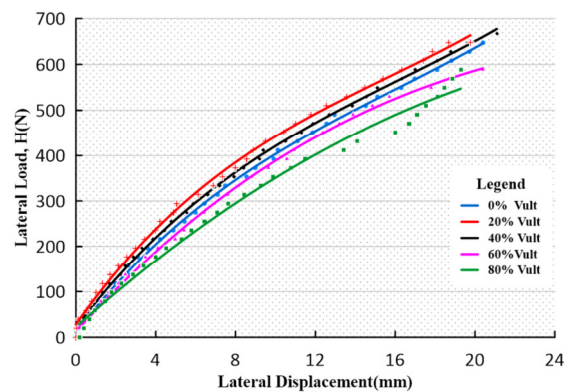


Fig. 13. Lateral load vs. lateral displacement curves for L/D=25.

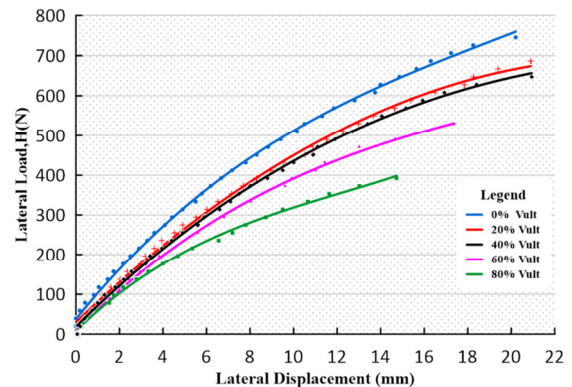


Fig. 14. Lateral load vs. lateral displacement curves for L/D=30.

On the other hand, as the vertical loads reach 40% Vult, a reduction in lateral capacity is noted compared to the condition with 20% vertical loads. Even so, the lateral capacity remains higher than that of pure lateral load in both cases. This phenomenon can be attributed to the development of bending moments caused by the increased vertical loads. Finally, when vertical loads increase to 60% Vult and 80% Vult, this results in an additional bending as the pile's lateral deformation advances. The last behavior is termed the P-Δ effect and it causes a decrease in lateral capacity (the P-Δ effect means that the increase of vertical load causes amplified lateral deflection because the force (P) acts on the displaced pile, creating larger bending moments. This can lead to a reduction in the lateral capacity of the pile). These results are in accordance with those in [40]. Conversely, in piles with a slenderness ratio of 30 (high L/D ratio, long pile) as shown in Figure 13 the P-Δ effect is more significant than the soil densification impact. Concurrently, the P-Δ effect is developed with increasing vertical loads, producing more pile deformation.

Figures 15-17 provide a concise overview of how vertical loads affect the lateral capacity when considering the slenderness ratio (L/D) of the piles. It is evident that the lateral deformation of the pile head diminishes as the vertical load escalates for vertical load smaller than 30% of the Vult. However, the lateral deformation at the pile head escalates as the vertical load increases to values greater than 30% of the Vult, in accordance with [42] in which the lateral deformation decreases with increasing vertical load until the vertical load

reached 50% Vult. Then the lateral deformation starts to increase with increasing vertical load.

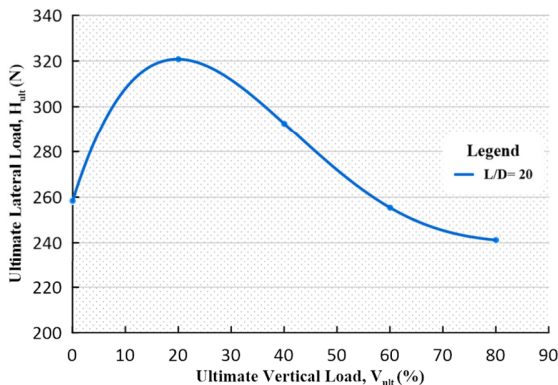


Fig. 15. Hult vs Vult percentage for L/D=20.

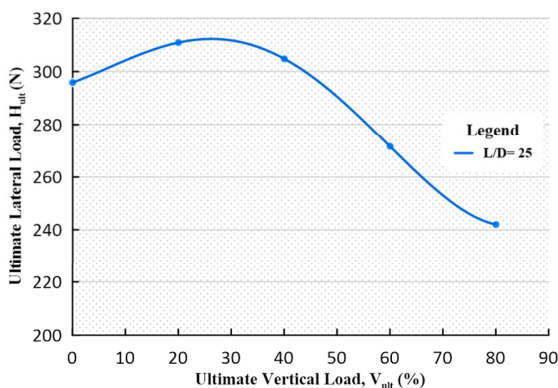


Fig. 16. Hult vs Vult percentage for L/D=25.

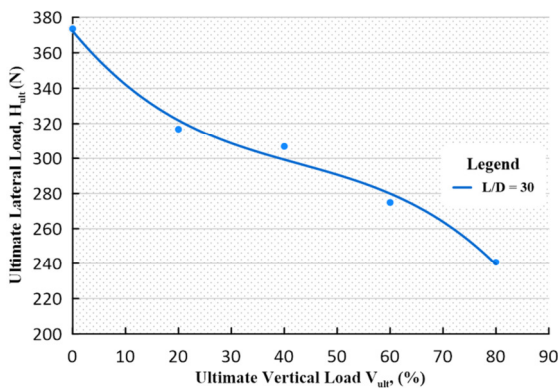


Fig. 17. Hult vs Vult percentage for L/D=30.

D. Lateral Displacement along the Pile Shaft

In order to determine the lateral displacement for various lateral load levels along the pile shaft, the images captured by PIV-camera for each test were analyzed. Accordingly, two photos were examined concerning the nearest value of the predicted ultimate lateral load, and two images were presented, i.e. before and after the ultimate lateral load. This section investigates the influence of the pile slenderness ratio (L/D) and vertical load level on the deformation behavior of a lateral

single pile, specifically focusing on how these two parameters affect lateral load-induced displacement.

1) Lateral Displacement under Pure Lateral Load along the Pile Shaft

Figure 18 shows the lateral displacement along the pile for all the considered L/D values.

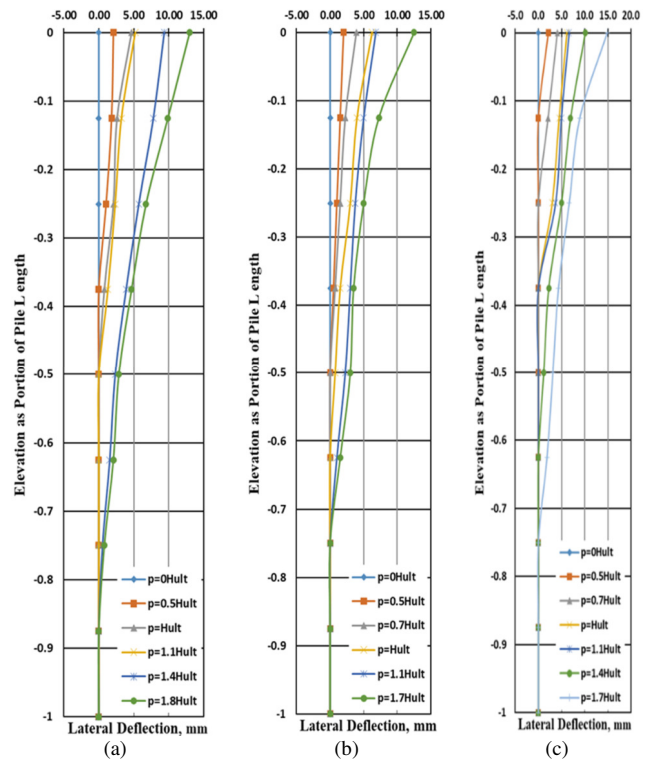


Fig. 18. Lateral displacement along the pile shaft under pure lateral load for piles with L/D equal to (a) 20, (b) 25, and (c) 30.

It is clear from Figure 18 that the lateral displacement along the pile shaft is proportionate to the lateral load. By taking into account the magnitude of the applied lateral load and the embedded length ratio, first, the displacement value is altered to a positive value at the pile top and then decreased to zero at a certain depth. In other words, regardless of the load level and for all embedded length ratios, the piles always experience their highest lateral displacement at the top and thereafter decline steadily until reaching zero. Figure 18 demonstrates that piles with L/D ratios of 20, 25, and 30 exhibits a fixation point (where the lateral displacement is zero) at an approximate distance of 1.8D, 2.5D, and 4.4D from the pile base, respectively. After the fixation point, all positive lateral displacements along the pile shaft drop to zero. It is noted that the position of the fixity point depends on and is sensitive to both the embedded length ratio and the lateral load level.

In general, at a certain lateral load level, the point of fixity is located far away from the pile base as L/D increases. In contrast, it moves toward the pile base for increasing lateral load and vice versa.

The observed behavior may be attributed to the increase in the confining pressure that surrounds the pile shaft, which constrains the lateral movement of the pile shaft near its base. For the same pile diameter, the soil confining pressure increased as the pile's embedment depth increased. Accordingly, when the lateral load level is low, the confining pressure absorbs a significant proportion of the applied lateral load, leading to no lateral displacements at the fixation point. On the other hand, as lateral load increases, the absorbed portion of the load decreases and the fixity point moves down to a certain depth depending on L/D and lateral load level as discussed above.

2) Lateral Displacement along the Pile Shaft for varying Vertical Load

The lateral displacements along the piles shaft were investigated for L/D values of 20, 25, and 30 under 20, 40, 60, and 80% of Vult. The subsequent sections analyze the outcomes for each pile in relation to the vertical load level.

Figure 19 displays the horizontal displacement along the pile shaft when exposed to 20% Vult. When 20 mm of displacement is specified, the deflection point (as measured from the pile base) for piles with L/D values of 20, 25, and 30 is observed to be around 3D, 1.3D, and 1.4D, respectively.

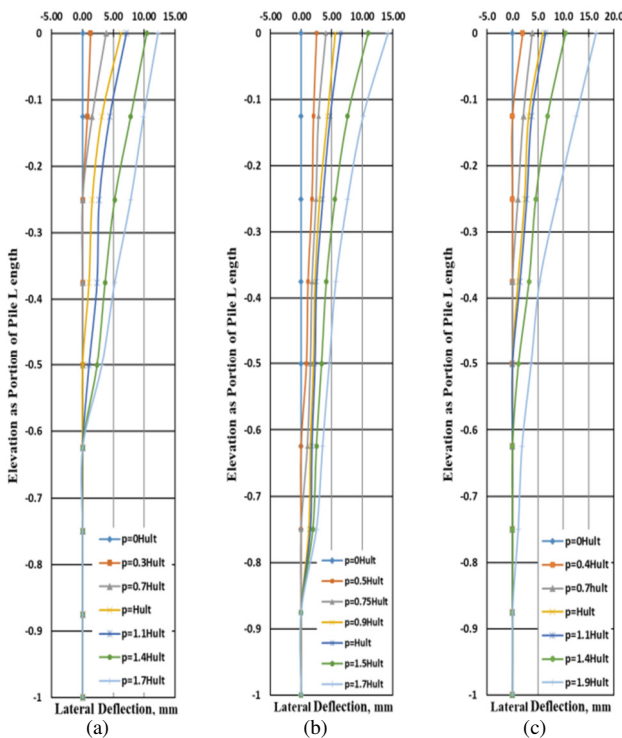


Fig. 19. Lateral displacement along the pile shaft under 20% Vult for piles with L/D equal to (a) 20, (b) 25, and (c) 30.

In Figure 20, the lateral displacement along the pile shaft is shown for 40% Vult. For a specified displacement of 20 mm that corresponds to the pile diameter at the pile head, the point of deflection, as measured from the base of the pile for piles with L/D values of 20, 25, and 30 is seen to be around 1D, 3.6D, and 3D, respectively.

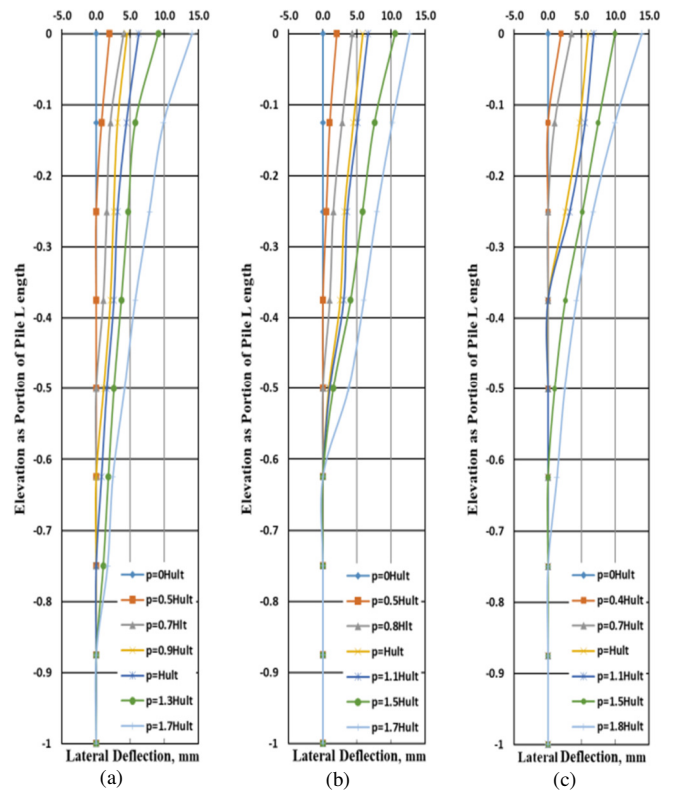


Fig. 20. Lateral displacement along the pile shaft under 40% Vult for piles with L/D equal to (a) 20, (b) 25, and (c) 30.

Figure 21 displays the pile shaft's lateral displacement at 60% Vult. For a specified displacement of 20 mm, the point of deflection, as determined from the pile base for piles with L/D of 20, 25, and 30 is seen to be around 3D, 6.2D, and 7.6D, respectively.

Figure 22 shows the lateral displacement along the pile shaft under 80% Vult. It is observed that the deflection point (measured from the pile base) for piles with L/D = 20, 25, and 30 is approximately 6D, 7.5D, and 9D for the specified displacement, which is equivalent to the pile diameter at a pile head.

The previous data illustrate that the displacement values for all slenderness ratios passed zero and turned positive for varying amounts of vertical load and L/D ratio depending on the magnitude of the imposed lateral load. However, regardless of the load level and embedded length ratios, the highest lateral displacement was obtained at the top of the piles and thereafter reduced to zero. Moreover, the slenderness ratio is a critical parameter that influences the deformation of a pile under a combined load. Observations indicate that, for all L/D ratios, a slight negative displacement is caused close to the pile base by the body of the pile rotating around the inflection point when the vertical load level is high (i.e. 80% Vult). The negative displacement is orientated in the opposite direction of the applied force, and its greatest magnitude occurs precisely at the base of the pile. The position of inflection points is influenced by the ratio of embedded length and remains nearly constant at a certain point.

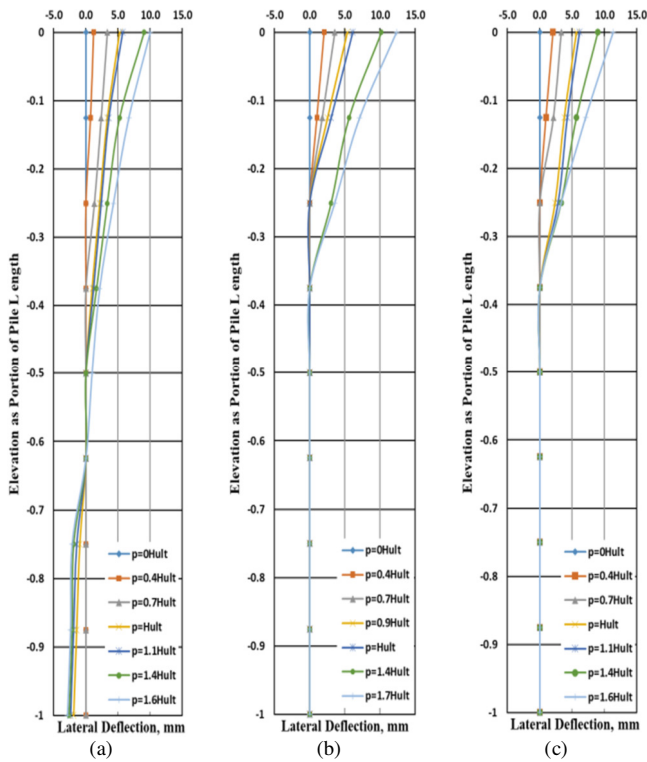


Fig. 21. Lateral displacement along the pile shaft under 60% Vult for piles with L/D equal to (a) 20, (b) 25, and (c) 30.

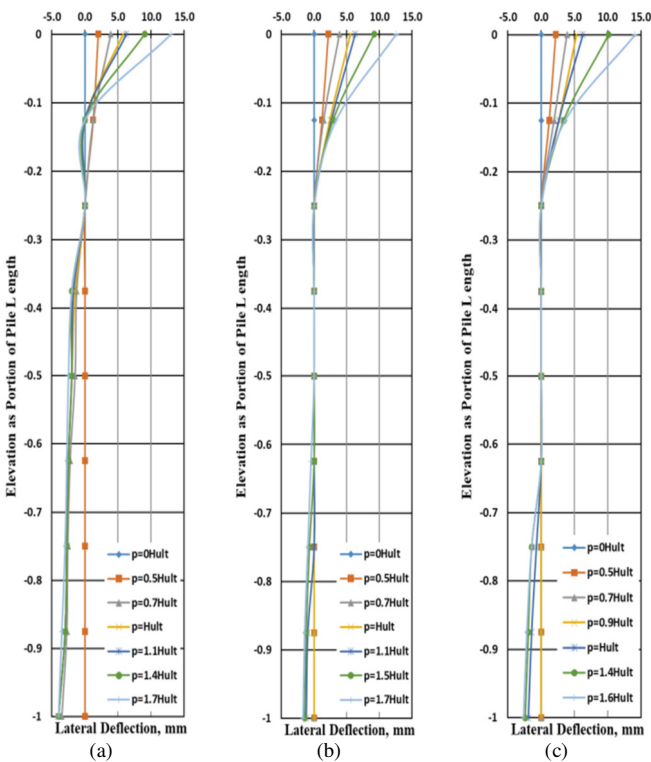


Fig. 22. Lateral displacement along the pile shaft under 80% Vult for piles with L/D equal to (a) 20, (b) 25, and (c) 30.

V. CONCLUSION AND FUTURE SCOPE

A series of experiments was performed to examine the impact of combined loads on the response of the soil-pile system, taking into account various pre-vertical loading conditions and L/D ratios. In previous studies, the responses of piles subjected to combined vertical and horizontal loads have been studied independently and subsequently superimposed in contemporary design methodology. This simple analytical method does not account for the coupling effects of the combined loads. The studies on this subject are limited and the findings thus far are inconclusive about the impact of vertical stresses on the horizontal reaction of piles. A critical aspect of the work involves determining the displacement along the piles, as the majority of research in this area is theoretical and relies on software applications. In this study, a wide range of loads was examined in contrast to prior studies, encompassing an extensive range of uncertainty that facilitates a thorough comprehension of pile behavior. This investigation's results allow for the following conclusions:

1. For short to intermediate piles, low vertical loads improve piles' lateral capacity due to the soil densification effect. However, excessive vertical loads reduce it due to the P-Δ effects.
2. In long piles, the P-Δ effect is more pronounced than the influence of soil densification, as it increases pile deformation by creating additional bending moments.
3. The piles consistently exhibit their maximum lateral displacement at the top, subsequently diminishing progressively until reaching zero when the piles are subjected to pure lateral load.
4. The position of the fixity point is sensitive to both the L/D ratio and the lateral load level. At low lateral loads, the confining pressure absorbs much of the load, keeping the displacement at the fixation point at zero. As the lateral load increases, less load is absorbed, causing the fixation point to shift deeper into the pile.
5. The slenderness ratio is a critical parameter that influences the deformation of a pile under a combined load.
6. For all L/D ratios, the pile body has a tendency to rotate around the inflection point and create a slight negative displacement close to the pile base when the vertical load level is high.

The results of the study at hand allow practitioners to get a thorough comprehension of pile behavior under combined vertical and lateral loading and to consider the combined effects of these loads in pile design, particularly for high-rise buildings and offshore constructions. For future work, the following are recommended:

1. A comparable investigation may be conducted on piles in cohesive soils or other sand densities.
2. The response of pile group exposed to combined loading conditions should be studied.

3. The behavior of individual or grouped piles subjected to dynamic loading with the PIV approach could be investigated.

## REFERENCES

- [1] A. Taha, M. Hesham El Naggari, and A. Turan, "Numerical modeling of the dynamic lateral behavior of geosynthetics-reinforced pile foundation system," *Soil Dynamics and Earthquake Engineering*, vol. 77, pp. 254–266, Oct. 2015, <https://doi.org/10.1016/j.soildyn.2015.05.017>.
- [2] A. Wakai, S. Gose, and K. Ugai, "3-D elasto-plastic finite element analyses of pile foundations subjected to lateral loading," *Soils and Foundations*, vol. 39, no. 1, pp. 97–111, 1999, <https://doi.org/10.3208/sandf.39.97>.
- [3] A. F. Elhakim, M. A. A. El Khouly, and R. Awad, "Three dimensional modeling of laterally loaded pile groups resting in sand," *HBRC Journal*, vol. 12, no. 1, pp. 78–87, Apr. 2016, <https://doi.org/10.1016/j.hbrj.2014.08.002>.
- [4] D. A. Brown and C.-F. Shie, "Numerical experiments into group effects on the response of piles to lateral loading," *Computers and Geotechnics*, vol. 10, no. 3, pp. 211–230, Jan. 1990, [https://doi.org/10.1016/0266-352X\(90\)90036-U](https://doi.org/10.1016/0266-352X(90)90036-U).
- [5] B. B. Broms, "Lateral Resistance of Piles in Cohesive Soils," *Journal of the Soil Mechanics and Foundations Division*, vol. 90, no. 2, pp. 27–63, Mar. 1964, <https://doi.org/10.1061/JSFEAQ.0000611>.
- [6] "Experimental study for lateral cyclic response of piled-raft foundation in multi-layer soil," <http://148.72.244.84:8080/jspui/handle/xmlui/8306>, 2020.
- [7] S. Prakash, "Behavior of Pile Groups Subjected to Lateral Loads," Ph.D. dissertation, University of Illinois, Urbana, IL, USA, 1962.
- [8] C. Anagnostopoulos and M. Georgiadis, "Interaction of Axial and Lateral Pile Responses," *Journal of Geotechnical Engineering*, vol. 119, no. 4, pp. 793–798, Apr. 1993, [https://doi.org/10.1061/\(ASCE\)0733-9410\(1993\)119:4\(793\)](https://doi.org/10.1061/(ASCE)0733-9410(1993)119:4(793)).
- [9] V. C. Maralappalle, M. B. Nadaf, S. Dutta, A. A. Zende, S. S. Mishra, and S. Charhate, "Load-settlement and skin friction behaviour of piles in dry sand: experimental and numerical study," *Sadhana*, vol. 49, no. 1, Dec. 2023, Art. no. 4, <https://doi.org/10.1007/s12046-023-02362-2>.
- [10] S. Karthigeyan, V. V. G. S. T. Ramakrishna, and K. Rajagopal, "Numerical Investigation of the Effect of Vertical Load on the Lateral Response of Piles," *Journal of Geotechnical and Geoenvironmental Engineering*, vol. 133, no. 5, pp. 512–521, May 2007, [https://doi.org/10.1061/\(ASCE\)1090-0241\(2007\)133:5\(512\)](https://doi.org/10.1061/(ASCE)1090-0241(2007)133:5(512)).
- [11] S. F. Ibraheem and M. K. Hatem, "Behavior of model group piles subjected to lateral soil movement in sand," *International Journal of GEOMATE*, vol. 21, no. 3, pp. 202–214, 2017, <https://doi.org/10.21660/2018.44.7208>.
- [12] L. B. Feagin, "Lateral Pile-Loading Tests," *Transactions of the American Society of Civil Engineers*, vol. 102, no. 1, pp. 236–254, Jan. 1937, <https://doi.org/10.1061/TACEAT.0004822>.
- [13] N. V. Zhukov and I. L. Balov, "Investigation of the effect of a vertical surcharge on horizontal displacements and resistance of pile columns to horizontal loads," *Soil Mechanics and Foundation Engineering*, vol. 15, no. 1, pp. 16–22, Jan. 1978, <https://doi.org/10.1007/BF02145324>.
- [14] B. F. Goryunov, "Analysis of piles subjected to the combined action of vertical and horizontal loads (discussion)," *Soil Mechanics and Foundation Engineering*, vol. 10, no. 1, pp. 10–13, Jan. 1973, <https://doi.org/10.1007/BF01706631>.
- [15] J. Lee, M. Prezzi, and R. Salgado, "Influence of Axial Load on the Lateral Capacity of Instrumented Steel Model Piles," *International Journal of Pavement Research and Technology*, vol. 6, no. 2, pp. 80–85, Mar. 2013.
- [16] C. Rha and E. Taciroglu, "Coupled Macroelement Model of Soil-Structure Interaction in Deep Foundations," *Journal of Engineering Mechanics*, vol. 133, no. 12, pp. 1326–1340, Dec. 2007, [https://doi.org/10.1061/\(ASCE\)0733-9399\(2007\)133:12\(1326\)](https://doi.org/10.1061/(ASCE)0733-9399(2007)133:12(1326)).
- [17] C. P. Aubeny, S. W. Han, and J. D. Murff, "Inclined load capacity of suction caissons," *International Journal for Numerical and Analytical Methods in Geomechanics*, vol. 27, no. 14, pp. 1235–1254, 2003, <https://doi.org/10.1002/nag.319>.
- [18] V. V. R. N. Sastry and G. G. Meyerhof, "Behaviour of flexible piles in layered sands under eccentric and inclined loads," *Canadian Geotechnical Journal*, vol. 31, no. 4, pp. 513–520, Aug. 1994, <https://doi.org/10.1139/t94-060>.
- [19] O. V. Karasev, G. P. Talanov, and S. F. Benda, "Investigation of the work of single situ-cast piles under different load combinations," *Soil Mechanics and Foundation Engineering*, vol. 14, no. 3, pp. 173–177, May 1977, <https://doi.org/10.1007/BF02092686>.
- [20] N. K. Jain, G. Ranjan, and G. Ramasamy, "Effect of vertical load on flexural behaviour of piles," *Geotechnical Engineering*, vol. 18, no. 2, pp. 185–204, Dec. 1987.
- [21] M. O. Karkush, "Impacts of Soil Contamination on the Response of Piles Foundation under a Combination of Loading," *Engineering, Technology & Applied Science Research*, vol. 6, no. 1, pp. 917–922, Feb. 2016, <https://doi.org/10.48084/etasr.616>.
- [22] W. Lu and G. Zhang, "Influence mechanism of vertical-horizontal combined loads on the response of a single pile in sand," *Soils and Foundations*, vol. 58, no. 5, pp. 1228–1239, Oct. 2018, <https://doi.org/10.1016/j.sandf.2018.07.002>.
- [23] L. C. Reese, S. T. Wang, J. A. Arrellaga, and J. Hendrix, *LPILE plus 3.0 for Windows*, Austin, TX, USA: Ensoft Inc., 1997.
- [24] M. McVay, T.-I. Shang, and R. Casper, "Centrifuge Testing of Fixed-Head Laterally Loaded Battered and Plumb Pile Groups in Sand," *Geotechnical Testing Journal*, vol. 19, no. 1, pp. 41–50, Mar. 1996, <https://doi.org/10.1520/GTJ11406J>.
- [25] A. Abdel-Mohti and Y. Khodair, "Analytical investigation of pile-soil interaction in sand under axial and lateral loads," *International Journal of Advanced Structural Engineering*, vol. 6, no. 1, Apr. 2014, Art. no. 54, <https://doi.org/10.1007/s40091-014-0054-5>.
- [26] B. Yuan, K. Xu, Y. Wang, R. Chen, and Q. Luo, "Investigation of Deflection of a Laterally Loaded Pile and Soil Deformation Using the PIV Technique," *International Journal of Geomechanics*, vol. 17, no. 6, Jun. 2017, Art. no. 04016138, [https://doi.org/10.1061/\(ASCE\)GM.1943-5622.0000842](https://doi.org/10.1061/(ASCE)GM.1943-5622.0000842).
- [27] M. Hajjalilue-Bonab, H. Azarnya-Shahgoli, and Y. Sojoudi, "Soil deformation pattern around laterally loaded piles," *International Journal of Physical Modelling in Geotechnics*, vol. 11, no. 3, pp. 116–125, Sep. 2011, <https://doi.org/10.1680/ijpmp.2011.11.3.116>.
- [28] C. Rahul, P. Saahas, V. S. Reddy, G. J. K. Alawadi, and A. H. Raide, "Lateral response of pile due to combined load under free and fixed conditions," *E3S Web of Conferences*, vol. 391, 2023, Art. no. 01219.
- [29] H. G. Poulos, "Behavior of Laterally Loaded Piles: II-Pile Groups," *Journal of the Soil Mechanics and Foundations Division*, vol. 97, no. 5, pp. 733–751, May 1971, <https://doi.org/10.1061/JSFEAQ.0001593>.
- [30] *ASTM D422-63 (2007), Standard Test Method for Particle Size Analysis of Soils*. West Conshohocken, PA, USA: ASTM International, 2007.
- [31] *ASTM D854-10 (2010), Standard Test Methods for Specific Gravity of Soil Solids by Water Pycnometer*. West Conshohocken, PA, USA: ASTM International, 2010.
- [32] *ASTM D4253-00 (2006), Standard Test Methods For Maximum Index Density And Unit Weight Of Soils Using A Vibratory Table*. West Conshohocken, PA, USA: ASTM International, 2006.
- [33] *ASTM D4253-16e1, Standard Test Methods for Maximum Index Density and Unit Weight of Soils Using a Vibratory Table*, West Conshohocken, PA, USA: ASTM International, 2019.
- [34] *ASTM D3080/D3080M – 11 (2004), Standard Test Method for Direct Shear Test of Soils Under Consolidated Drained Conditions*. West Conshohocken, PA, USA: ASTM International, 2004.
- [35] *ASTM D7181-20, Standard Test Method for Consolidated Drained Triaxial Compression Test for Soils*, West Conshohocken, PA, USA: ASTM International, 2020.
- [36] D. Al-Jeznawi, I. B. M. Jais, B. S. Albusoda, and N. Khalid, "The slenderness ratio effect on the response of closed-end pipe piles in liquefied and non-liquefied soil layers under coupled static-seismic

- loading." *Journal of the Mechanical Behavior of Materials*, vol. 31, no. 1, pp. 83–89, Jan. 2022, <https://doi.org/10.1515/jmbm-2022-0009>.
- [37] *D 1143/D 1143M – 07 (2007), Standard Test Methods for Deep Foundations Under Static Axial Compressive Load*. West Conshohocken, PA, USA: ASTM International, 2007.
- [38] *ASTM D3966-90, Standard Test Method for Piles Under Lateral Loads*, West Conshohocken, PA, USA: ASTM International, 1995.
- [39] K. C. Birid, "Evaluation of Ultimate Pile Compression Capacity from Static Pile Load Test Results," in *Advances in Analysis and Design of Deep Foundations*, M. Abu-Farsakh, K. Alshibli, and A. Puppala, Eds. New York, NY, USA: Springer, 2018, pp. 1–14.
- [40] R. Adel and R. R. Shakir, "Evaluation of Static Pile Load Test Results of Ultimate Bearing Capacity by Interpreting Methods," *IOP Conference Series: Earth and Environmental Science*, vol. 961, Jan. 2022, Art. no. 012013, <https://doi.org/10.1088/1755-1315/961/1/012013>.
- [41] *ASTM D3966/D3966M, Standard Test Methods for Deep Foundation Elements Under Static Lateral Load*. West Conshohocken, PA, USA: ASTM International, 2022.
- [42] L. Mu, X. Kang, K. Feng, M. Huang, and J. Cao, "Influence of vertical loads on lateral behaviour of monopiles in sand," *European Journal of Environmental and Civil Engineering*, vol. 22, no. sup1, pp. s286–s301, Aug. 2018, <https://doi.org/10.1080/19648189.2017.1359112>.